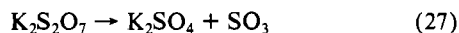


**Figure 3.** Thermogravimetric analysis of potassium pyrosulfate, and of transition-metal oxides with potassium pyrosulfate, in the ternary sulfate eutectic under nitrogen: A (○), 0.33 *m* K<sub>2</sub>S<sub>2</sub>O<sub>7</sub>; B (×), 0.33 *m* TiO<sub>2</sub> + 0.33 *m* K<sub>2</sub>S<sub>2</sub>O<sub>7</sub>; C (△), 0.33 *m* MoO<sub>3</sub> + 0.33 *m* K<sub>2</sub>S<sub>2</sub>O<sub>7</sub>; D (□), 0.33 *m* WO<sub>3</sub> + 0.33 *m* K<sub>2</sub>S<sub>2</sub>O<sub>7</sub>; E (■), 0.33 *m* Nb<sub>2</sub>O<sub>5</sub> + 0.33 *m* K<sub>2</sub>S<sub>2</sub>O<sub>7</sub>; F (▽), 0.33 *m* Ta<sub>2</sub>O<sub>5</sub> + 0.33 *m* K<sub>2</sub>S<sub>2</sub>O<sub>7</sub>.

higher than with only pyrosulfate in the sulfate melt (cf. Figure 3, curve A) and thus in terms of the sulfuric acid catalyst that sulfur trioxide was considerably stabilized in the presence of these transition-metal oxides. Though in each case the appropriate amount of sulfur trioxide was evolved at a sufficiently high temperature, i.e.



(calculated weight loss 80 g/mol of K<sub>2</sub>S<sub>2</sub>O<sub>7</sub>), the order of stabilization varied considerably with temperature, being Ta < W < Ti < Nb < Mo at 500 °C but W < Ta < Mo < Ti < Nb at 700 °C. The delay of weight loss with molybdenum and tungsten oxide to 430 °C (curves C and D) indicated that interaction of pyrosulfate and the metal oxide had occurred below 340 °C (the decomposition temperature of K<sub>2</sub>S<sub>2</sub>O<sub>7</sub> in the sulfate eutectic) while the closely similar decomposition of pyrosulfate alone (curve A) and with tantalum oxide (curve F) up to 500 °C suggested that interaction only commenced at this temperature. Before decomposition, the colorless solutions presumably contained nominally cationic transition-metal species, though by analogy with their aqueous chemistry these may not have been monomeric (e.g. MoO<sub>2</sub><sup>2+</sup>) but polymeric (e.g. (TiO)<sub>n</sub><sup>2+</sup>). In either case their thermal stability (cf. Figure 1 and Table I) suggests that considerable coordination by sulfate anions would be expected, with the metals probably also joined by oxo bridges. Such chains, or three-dimensional polymers, (sulfates can be bidentate and bridging), which are such a noteworthy feature of vanadium solutions in sulfate melts, may well be important in the performance of the sulfuric acid catalysts.

**Acknowledgment.** Grateful thanks are expressed to the SERC and to ISC Chemicals, Avonmouth, U.K., for CASE scholarships to R.I.D. and D.J.R.

**Registry No.** Li<sub>2</sub>SO<sub>4</sub>, 10377-48-7; Na<sub>2</sub>SO<sub>4</sub>, 7757-82-6; K<sub>2</sub>SO<sub>4</sub>, 7778-80-5; Cr<sub>2</sub>O<sub>3</sub>, 1308-38-9; TiO<sub>2</sub>, 13463-67-7; MnO<sub>2</sub>, 1313-13-9; Nb<sub>2</sub>O<sub>5</sub>, 1313-96-8; WO<sub>3</sub>, 1314-35-8; Ta<sub>2</sub>O<sub>5</sub>, 1314-61-0; MoO<sub>3</sub>, 1313-27-5; Cr<sub>2</sub>(SO<sub>4</sub>)<sub>3</sub>, 10101-53-8; MnSO<sub>4</sub>, 7785-87-7; FeSO<sub>4</sub>, 7720-78-7; Fe<sub>2</sub>(SO<sub>4</sub>)<sub>3</sub>, 10028-22-5; CoSO<sub>4</sub>, 10124-43-3; NiSO<sub>4</sub>, 7786-81-4; CuSO<sub>4</sub>, 7758-98-7; K<sub>2</sub>S<sub>2</sub>O<sub>7</sub>, 7790-62-7; Na<sub>2</sub>CO<sub>3</sub>, 497-19-8.

Contribution from the Department of Chemistry, School of Science and Engineering, Waseda University, Shinjuku-ku, Tokyo 160, Japan

## Resonance Raman and Surface-Enhanced Resonance Raman Scattering Studies on Electrochemical Redox Processes of Iron Tetrakis(*N*-methyl-4-pyridiniumyl)porphine

TOSHIYA KOYAMA, MINORU YAMAGA, MUNSOK KIM, and KOICHI ITOH\*

Received December 18, 1984

The electrochemical reduction processes of iron(III) tetrakis(*N*-methyl-4-pyridiniumyl)porphine (Fe<sup>III</sup>TMPyP) at pH 1.0 (in 0.1 *N* H<sub>2</sub>SO<sub>4</sub>) and 10.5 (in 0.1 *N* K<sub>2</sub>SO<sub>4</sub> + KOH) were followed by resonance Raman spectroscopy. On conversion from the ferric complex to the ferrous one at pH 1.0 the Raman band mainly due to the C<sub>β</sub>-C<sub>β</sub> stretching vibration and that due to the C<sub>α</sub>-N stretching vibration shift from 1557 to 1547 cm<sup>-1</sup> and from 1363 to 1345 cm<sup>-1</sup>, respectively. Similar frequency shifts were observed for the reduction at pH 10.5. From these results it was concluded that the reduction of the metalloporphine proceeds in a high-spin state at both pHs. The redox processes of FeTMPyP adsorbed at Ag electrode surfaces were also studied by surface-enhanced resonance Raman spectroscopy. The SERS + RRS spectra observed at -0.1 and -0.35 V (vs. Ag/AgCl) for the adsorbate from the solution of FeTMPyP in 0.1 *M* Na<sub>2</sub>SO<sub>4</sub> (pH 5.6) are almost the same as the RRS spectra of the ferric and ferrous porphines in the bulk solution, respectively. At pH 1.0 (in 0.1 *N* H<sub>2</sub>SO<sub>4</sub>) the adsorbate, which gives rise to the SERS + RRS spectrum characteristic of the ferrous complex at -0.15 V, shows a marked change in the surface spectrum on sweeping the electrode potential to +0.135 V. This change can be interpreted as arising from an elimination process of the central iron atom from the complex. The surface spectra observed under various conditions at pH 1.0 proved that a reversible elimination-incorporation process of the central iron atom is taking place at the electrode surface in the potential range of -0.15 to +0.135 V.

### Introduction

Electrochemical properties of metalloporphines have been studied by a variety of methods.<sup>1</sup> Notably iron porphyrins in bulk solutions and those on electrode surfaces are of special interest because of their biological importance and catalytic properties.<sup>2</sup> Several recent publications indicated that resonance Raman scattering (RRS) spectroscopy with the combined use of an electrochemical system is very useful for elucidating the structural changes accompanied by the redox reactions of metalloporphines.<sup>3</sup> Surface-enhanced resonance Raman scattering (SERS + RRS) spectroscopy is expected to be very useful to

understand the reactions taking place on electrode surfaces.<sup>4</sup> The application of these methods has been previously demonstrated for water-soluble porphines such as *meso*-tetrakis(4-sulfonato-phenyl)porphine (TSPP),<sup>5,6</sup> *meso*-tetrakis(4-carboxyphenyl)por-

\* To whom correspondence should be addressed.

- (1) Dolphin, D., Ed. "The Porphyrins"; Academic Press: New York, 1966; Vol. 3.
- (2) Kadish, K. M., Ed. "Electrochemical and Spectrochemical Studies of Biological Redox Components"; American Chemical Society: Washington, D.C., 1982; Adv. Chem. Ser. No. 201.
- (3) For example, see: Yamaguchi, H.; Soeta, A.; Toeda, H.; Itoh, K. *J. Electroanal. Chem. Interfacial Electrochem.* **1983**, *159*, 347.
- (4) Chang, R. K.; Furtak, T. E., Eds. "Surface Enhanced Raman Scattering"; Plenum Press: New York, London, 1982.
- (5) Cotton, T. M.; Schultz, S. G.; Van Duyne, R. P. *J. Am. Chem. Soc.* **1982**, *104*, 6582.
- (6) Itabashi, M.; Kato, K.; Itoh, K. *Chem. Phys. Lett.* **1983**, *97*, 528.

phine (TCPP),<sup>5</sup> and *meso*-tetrakis(*N*-methyl-4-pyridiniumyl)porphine (TMPyP)<sup>7</sup> and for several hemoproteins.<sup>8,9</sup>

In this paper we followed the change in the RRS (or more rigorously preresonance Raman scattering) spectra due to the electrochemical reduction of a water-soluble iron porphine, iron tetrakis(*N*-methyl-4-pyridiniumyl)porphine (This is abbreviated Fe<sup>III/II</sup>TMPyP<sup>5+/4+</sup>, omitting the counterion.), under various conditions. The electrochemistry of the water-soluble iron complex has been extensively studied by Forshey and Kuwana<sup>10,11</sup> with use of optically coupled electrochemical techniques. According to these authors, four ferric species (three monomeric and one dimeric) and two ferrous species (both monomeric) are sufficient to explain the electrochemical processes of the metalloporphine in the pH region of 1–13. The RRS studies give some insight into the structures of these species. In addition to the studies for the bulk solutions we investigated also the potential dependence of the SERS + RRS spectra of Fe<sup>III/II</sup>TMPyP<sup>5+/4+</sup> adsorbed on Ag electrodes under conditions similar to those employed by the bulk-solution studies. When the surface spectra are compared with the RRS spectra of the corresponding samples, we can obtain some information about how the adsorption to the Ag electrode surface affects the structure of the water-soluble metalloporphine. The results of these studies will be presented in the following.

### Experimental Section

**Materials.** TMPyP was obtained from Midcentury Co. as its iodide salt and used without any purification process. Fe<sup>III</sup>TMPyP<sup>5+</sup> was prepared as a chloride salt form by following the method of Pasternack et al.<sup>12</sup> Other chemicals are reagent grade and obtained as commercial products.

**Measurement of RRS and Optical Absorption Spectra of Fe<sup>III</sup>TMPyP<sup>5+</sup> and Its Controlled-Potential Electrolysis Products.** A three-electrode cell was used for controlled-potential electrolysis of Fe<sup>III</sup>TMPyP<sup>5+</sup> under various conditions. Using the same electrochemical cell, we measured the RRS spectra as well as the absorption spectra of the electrolysis products. The cell design and the method of the measurements have already been reported in detail.<sup>3</sup> In the present study a gold mesh (mesh 100, 1 cm × 2.5 cm) was used as the working electrode. All the RRS spectra were observed with the excitation wavelength of 457.9 nm. The electrode potentials were measured with the use of a silver-silver chloride (in saturated KCl) reference electrode. Sample solutions were deoxygenated by bubbling highly purified argon gas prior to use.

**Measurement of SERS + RRS Spectra.** The SERS + RRS spectra of Fe<sup>III/II</sup>TMPyP<sup>5+/4+</sup> under various conditions were measured with 457.9-nm excitation by using the same electrochemical systems and cell as those described in the previous papers.<sup>6,7</sup> The cell contains a platinum-wire counter electrode, a silver-silver chloride (in saturated KCl) reference electrode, and a polycrystalline Ag working electrode (1.1 cm<sup>2</sup> exposed surface area with the remainder masked with a heat-shrinkable tube). The working electrode was mechanically polished with 0.3- and 0.06- $\mu$ m Al<sub>2</sub>O<sub>3</sub> abrasives successively, rinsed with distilled water, and anodized by the following procedure. First, the electrode potential was potentiostated at 0.6 V (vs. Ag/AgCl). After 45 mC cm<sup>-2</sup> of charge was passed through the Ag electrode, the potential was altered slowly to a value at which a surface spectrum was taken. The Raman spectrophotometer and the excitation source are the same as those used for the RRS spectral measurement. All the sample solutions were prepared by using deionized and distilled water and deoxygenated by bubbling high-purity argon gas prior to use.

### Results and Discussion

**RRS and Absorption Spectra of Fe<sup>III/II</sup>TMPyP<sup>5+/4+</sup> at pH 1.0 and 10.5.** Figure 1A presents the absorption spectra observed during controlled-potential electrolysis at -0.2 V of 1.0 × 10<sup>-4</sup> M Fe<sup>III</sup>TMPyP in 0.1 N H<sub>2</sub>SO<sub>4</sub>. The arrows indicate the direction

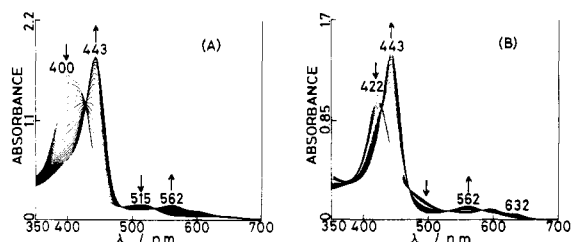


Figure 1. Absorption spectra recorded during incremental charge addition for the reduction of Fe<sup>III</sup>TMPyP at pH 1.0 (A) and at pH 10.5 (B) (see text).

of the change of absorbance during the reduction. According to Forshey and Kuwana<sup>10,11</sup> the  $E_{0.85}$  value for the Fe<sup>III</sup>TMPyP reduction is 0.18 ( $\pm 0.01$ ) V (vs. NHE) in 0.1 N H<sub>2</sub>SO<sub>4</sub> and the observed spectral change can be ascribed to the reaction

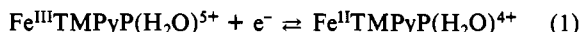
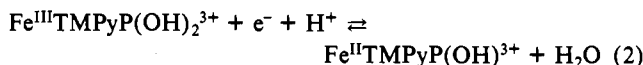
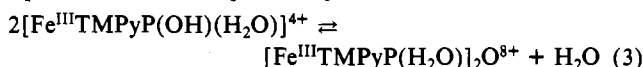


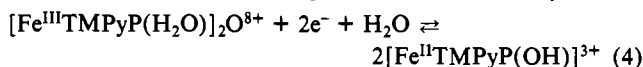
Figure 1B shows the absorption spectra obtained during the controlled-potential electrolysis at -0.35 V of a 1.0 × 10<sup>-4</sup> M Fe<sup>III</sup>TMPyP solution with pH 10.5 (The pH value was adjusted by adding a KOH solution to the sample in 0.1 N K<sub>2</sub>SO<sub>4</sub>). It has been proposed<sup>11</sup> that at pH above 8 the ferric porphine should show a reduction process that can be summarized as



It has also been reported that in alkaline solutions the ferric porphine shows a monomer-dimer equilibrium. In their electrochemical studies, Forshey and Kuwana<sup>10</sup> proposed that the equilibrium can be expressed by



In fact the cyclic voltammogram observed for Fe<sup>III</sup>TMPyP at pH 10.5 shows a cathodic wave at -0.52 V due to the reduction of a dimer in addition to a wave at -0.30 V ascribable to the reduction of the dihydroxy monomer, which is followed by the reaction represented by eq 2. The dimer, when reduced, rapidly dissociates to ferrous monomers following the reaction written by



As Figure 1B shows, the solution of the ferric porphine (Presumably, the solution contains both the dihydroxy monomer, Fe<sup>III</sup>TMPyP(OH)<sub>2</sub><sup>3+</sup>, and the dimer, [Fe<sup>III</sup>TMPyP(H<sub>2</sub>O)<sub>2</sub>]<sub>2</sub>O<sup>8+</sup>.) gives an absorption maximum at 422 nm and another maximum at approximately 600 nm while the ferrous porphine has maxima at 443 and 562 nm. The absorption spectrum of the reduction product at pH 10.5 (Figure 1B) is virtually identical with that observed for the ferrous porphine in 0.1 N H<sub>2</sub>SO<sub>4</sub> (Figure 1A).

By using the same electrochemical cell as that used for the measurement of the absorption spectra in Figure 1, we measured the RRS spectra of Fe<sup>III</sup>TMPyP at pH 1.0 and 10.5 and those of their reduction products, the results being shown in Figure 2. From parts A and B of Figure 2 it is recognized that, on conversion from Fe<sup>III</sup>TMPyP to Fe<sup>II</sup>TMPyP at pH 1.0, the Raman bands at 1363 and 1557 cm<sup>-1</sup> observed for the ferric complex shift to 1345 and 1547 cm<sup>-1</sup>, respectively. The bands near 1350 and 1550 cm<sup>-1</sup> can be assigned mainly due to the C<sub>α</sub>-N and C<sub>β</sub>-C<sub>β</sub> stretching vibrations, respectively, according to the extensive study done by Burke et al.<sup>13,14</sup> on Fe<sup>III</sup>(TPP)Cl (TPP = tetraphenylporphine) and its  $\mu$ -oxo dimer. Chottard et al.<sup>15</sup> classified the former and the latter bands as band A and band D, respectively, in their study of the RRS spectra of Fe<sup>II/III</sup>TPP(L)(L') (L and

- (7) Itabashi, M.; Masuda, T.; Itoh, K. *J. Electroanal. Chem. Interfacial Electrochem.* **1984**, *165*, 265.
- (8) Cotton, T. M.; Schultz, S. G.; Van Duyne, R. P. *J. Am. Chem. Soc.* **1980**, *102*, 7960.
- (9) Cotton, T. M.; Timkovich, R.; Van Duyne, R. P. *FEBS Lett.* **1981**, *133*, 39.
- (10) Forshey, P. A.; Kuwana, T. *Inorg. Chem.* **1981**, *20*, 693.
- (11) Forshey, P. A.; Kuwana, T.; Kobayashi, N.; Osa, T. In "Electrochemical and Spectrochemical Studies of Biological Redox Components"; Kadish, K. M., Ed.; American Chemical Society: Washington, D.C., 1982; Adv. Chem. Ser. No. 201, pp 601–624.
- (12) Pasternack, R. F.; Howard, L.; Malek, P.; Spencer, C. *J. Inorg. Nucl. Chem.* **1977**, *39*, 1865.

- (13) Burke, J. M.; Kincaid, J. R.; Spiro, T. G. *J. Am. Chem. Soc.* **1978**, *100*, 6077.
- (14) Burke, J. M.; Kincaid, J. R.; Peters, S.; Gagne, R. R.; Collman, J. P.; Spiro, T. G. *J. Am. Chem. Soc.* **1978**, *100*, 6083.
- (15) Chottard, G.; Battioni, J.-P.; Lange, M.; Mansuy, D. *Inorg. Chem.* **1981**, *20*, 1718.

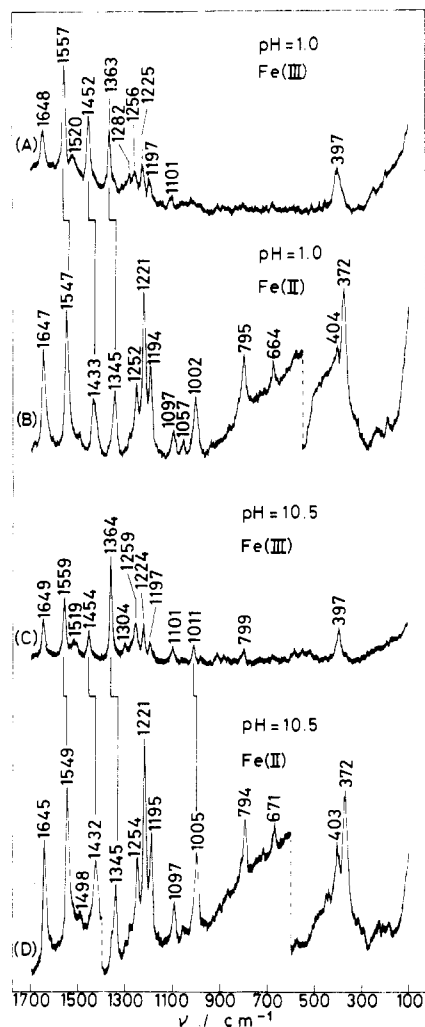


**Figure 2.** RRS spectra of  $\text{Fe}^{\text{III}}\text{TMPyP}$  (A) and  $\text{Fe}^{\text{II}}\text{TMPyP}$  (B) at pH 1.0, and RRS spectra of  $\text{Fe}^{\text{III}}\text{TMPyP}$  (C) and  $\text{Fe}^{\text{II}}\text{TMPyP}$  (D) at pH 10.5 (see text; sample concentration  $(2.0\text{--}3.0) \times 10^{-4}$ , excitation wavelength 457.9 nm).

$\text{L}'$  denote various ligands.). According to Chottard et al.,<sup>15</sup> the ferric complexes in a high-spin state give rise to bands A and D at 1360–1363 and 1545–1554  $\text{cm}^{-1}$ , respectively, while the ferric complex in a low-spin state (e.g.,  $\text{Fe}^{\text{III}}\text{TPP}(\text{Im})_2$ ) gives these bands at 1370 and 1568  $\text{cm}^{-1}$ , respectively. Further, they indicated that the ferrous tetraphenylporphines in a low-spin state show bands A and D in the 1355–1369- and 1560–1572- $\text{cm}^{-1}$  regions, respectively, while the ferrous complex in a high-spin state (e.g.,  $\text{Fe}^{\text{II}}\text{TPP}(2\text{-CH}_3\text{Im})_2$ ) gives the corresponding bands at 1345 and 1542  $\text{cm}^{-1}$ , respectively. On the basis of these data we can conclude from the above-mentioned frequency shifts of bands A and D in Figure 2A,B that both  $\text{Fe}^{\text{III}}\text{TMPyP}$  and  $\text{Fe}^{\text{II}}\text{TMPyP}$  exist in a high-spin state at pH 1.0.

With regard to the coordination number Forshey et al.<sup>11</sup> presented magnetic circular dichroism spectroscopic results on  $\text{Fe}^{\text{II}}\text{TMPyP}$  as a reliable indication of the five-coordinate structure of the ferrous complex in acidic solutions as proposed in eq 1. These authors, however, did not give any evidence in support of the five-coordinate structure of  $\text{Fe}^{\text{III}}\text{TMPyP}$  in eq 1. On the other hand, in the presence of weak-field ligands such as  $\text{H}_2\text{O}$  and dimethyl sulfoxide, iron(III) tetraphenylporphines ( $\text{Fe}^{\text{III}}\text{TPP}$ ) generally take a six-coordinate high-spin state; e.g.,  $\text{Fe}^{\text{III}}\text{TPP}(\text{H}_2\text{O})_2\text{ClO}_4$ <sup>16</sup> and  $\text{Fe}^{\text{III}}\text{TPP}(\text{Me}_2\text{SO})_2\text{ClO}_4$ .<sup>16</sup> These complexes have an in-plane iron atom with an expanded porphine core. According to Spiro et al.<sup>17</sup> and Chottard et al.,<sup>15</sup> the bis(dimethyl

sulfoxide) complex of  $\text{Fe}^{\text{III}}\text{TPP}$  gives rise to the  $\text{C}_\alpha\text{-N}$  (band A) and  $\text{C}_\beta\text{-C}_\beta$  (band D) stretching vibrations near 1360 and 1550  $\text{cm}^{-1}$ , respectively. These frequencies are similar to those of the corresponding bands observed for  $\text{Fe}^{\text{III}}\text{TMPyP}$  at pH 1.0 (Figure 2A). In addition, the RRS spectrum observed for  $\text{Fe}^{\text{III}}\text{TMPyP}$  in dimethyl sulfoxide (Presumably, the complex takes a six-coordinate high-spin state.) by the 457.9-nm excitation shows the  $\text{C}_\alpha\text{-N}$  and  $\text{C}_\beta\text{-C}_\beta$  stretching vibrations at 1362 and 1557  $\text{cm}^{-1}$ , respectively, which are again almost identical with the corresponding frequencies observed in Figure 2A. On the basis of these results we concluded that  $\text{Fe}^{\text{III}}\text{TMPyP}$  at pH 1.0 takes a six-coordinate high-spin state (i.e.,  $\text{Fe}^{\text{III}}\text{TMPyP}(\text{H}_2\text{O})_2^{5+}$ ) instead of the monoquo complex in eq 1.

It is also noticed from Figure 2A,B that, on conversion from the ferric to the ferrous porphine, the Raman band at 1452  $\text{cm}^{-1}$  shifts to 1433  $\text{cm}^{-1}$  and a prominent band appears at 372  $\text{cm}^{-1}$ . The bands at 1452 and 1433  $\text{cm}^{-1}$  are polarized bands, and according to Burke et al.,<sup>13</sup> they are mainly due to the  $\text{C}_\alpha\text{-C}_\beta$  stretching vibration of the porphine ring. The polarized band at 372  $\text{cm}^{-1}$ , characteristic of the ferrous porphine, can be assigned to a deformation vibration of the porphine ring that is shifted from the 397- $\text{cm}^{-1}$  band observed for the ferric porphine (Presumably the 397- $\text{cm}^{-1}$  band in Figure 2A is composed of two components. On reduction the one component shifts to 372  $\text{cm}^{-1}$  and the other, which does not shift its frequency on reduction, may be a counterpart of the 404- $\text{cm}^{-1}$  band in Figure 2B.). Stong et al.<sup>18</sup> studied the RRS spectra of various metallotetraphenylporphines and revealed that the polarized  $\text{C}_\beta\text{-C}_\beta$  (near 1550  $\text{cm}^{-1}$ ) and  $\text{C}_\alpha\text{-C}_\beta$  (near 1450  $\text{cm}^{-1}$ ) stretching vibrations exhibit a linear correlation with porphine core size (the  $\text{C}_1\text{-N}$  length). On the basis of this result it can be concluded from the frequency shifts of these modes caused by the ferric to ferrous transformation of  $\text{Fe}^{\text{III}}\text{TMPyP}$  at pH 1.0 (1557  $\rightarrow$  1547 and 1452  $\rightarrow$  1433  $\text{cm}^{-1}$ ; see Figure 2A,B) that the transformation results in an appreciable expansion of the porphine core of the iron complex. The deformation vibration around 380  $\text{cm}^{-1}$  is expected to be sensitive to the structure of the porphine, and the shift to the low-frequency side (397  $\rightarrow$  372  $\text{cm}^{-1}$ ; see Figure 2A,B) of this vibration may be another core-expansion marker.

From comparison of parts C and D with parts A and B of Figure 2 it is clear that the RRS spectra of the ferric and ferrous porphines at pH 10.5 are almost identical with the spectra of the complexes with the corresponding oxidation state at pH 1.0. Therefore, at pH 10.5 the ferric porphine exists in a high-spin state and its reduction proceeds with retention of its spin state. Further, the above-mentioned result indicates that the structures of the ferric and ferrous porphines at pH 10.5 are almost identical with those of the corresponding metalloporphines at pH 1.0. Goff and Morgan<sup>19</sup> studied the pH dependence of the magnetic moment of the ferric porphine and reported that the complex undergoes a high-spin to low-spin transition at pH above 5. Then, with regard to the spin state of the porphine at alkaline pH there is a discrepancy between the result of the RRS study and that of the magnetic moment. In order to elucidate this point, we made detailed RRS measurements on the ferric porphine at various pHs. The results, however, did not show any evidence that the sample takes a low-spin state at alkaline pH. The discrepancy may be ascribed to the differences in components of aqueous media, coexisting ions, ionic strength, and sample concentration between the RRS and the magnetic moment studies. As mentioned above, it has been proposed that the ferric porphine at alkaline pH should show a dimer-monomer equilibrium.<sup>10,11</sup> According to Burke et al.,<sup>13</sup> the  $\mu$ -oxo dimer  $[\text{Fe}^{\text{III}}\text{TPP}]_2\text{O}$  gives rise to a totally symmetric  $\text{Fe-O-Fe}$  stretching vibration at 363  $\text{cm}^{-1}$ . The RRS spectrum in Figure 2C does not show any band in this frequency region. We tried also to observe the spectrum with 514.5-nm excitation. Although the observed spectrum was of poor quality, it did not show any feature in the frequency region. These results indicate

(16) Mashiko, T.; Kastner, M. E.; Spaltalian, K.; Scheidt, W. R.; Reed, C. A. *J. Am. Chem. Soc.* **1978**, *100*, 6354.

(17) Spiro, T. G.; Stong, J. D.; Stein, P. *J. Am. Chem. Soc.* **1979**, *101*, 2648.

(18) Stong, J. D.; Spiro, T. G.; Kubaska, R. J.; Shupack, S. I. *J. Raman Spectrosc.* **1980**, *9*, 312.

(19) Goff, H.; Morgan, L. O. *Inorg. Chem.* **1976**, *15*, 3180.

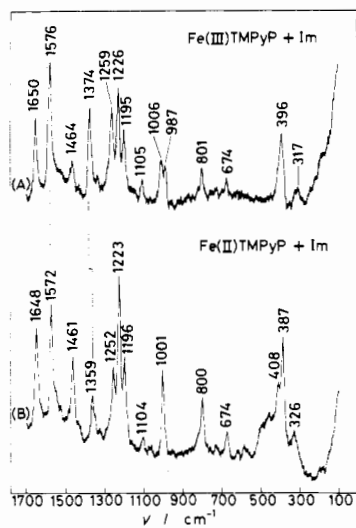


**Figure 3.** RRS spectra of  $\text{Fe}^{\text{III}}\text{TMPyP}(\text{Im})_2$  (A) and  $\text{Fe}^{\text{II}}\text{TMPyP}(\text{Im})_2$  (B) at pH 5.6 (see text; sample concentration ca.  $1.5 \times 10^{-4}$  sample + ca. 0.6 M imidazole, excitation wavelength 457.9 nm).

that at pH 10.5 the concentration of the  $\mu$ -oxo dimer  $[\text{Fe}^{\text{III}}\text{TMPyP}(\text{H}_2\text{O})_2]_2\text{O}^{8+}$  is too small to be detected by RRS spectroscopy.

**RRS Spectra of  $\text{Fe}^{\text{III/II}}\text{TMPyP}^{5+/4+}$  in a Low-Spin State.** It is a well-established fact that ferric and ferrous porphines take a low-spin state when nitrogenous ligands such as pyridine and imidazole take two axial sites of the complexes.<sup>14,15</sup> Weinraub et al.<sup>20</sup> studied absorption spectra of  $\text{Fe}^{\text{III/II}}\text{TMPyP}^{5+/4+}$  in the presence of imidazole and reported the spectra of the complexes in a low-spin state. Figure 3A shows the RRS spectrum of ca.  $1.5 \times 10^{-4}$  M  $\text{Fe}^{\text{III}}\text{TMPyP}(\text{Im})_2$  in 0.1 N  $\text{Na}_2\text{SO}_4$  + 0.6 M imidazole and Figure 3B the RRS spectrum of the reduction product of a controlled-potential electrolysis at  $-0.2$  V of the same sample solution. The absorption spectrum of the sample solution that gives the RRS spectrum shown in Figure 3A was confirmed to be identical with that ascribed by Weinraub et al.<sup>20</sup> to the ferric porphine in the low-spin state. As Figure 3A shows,  $\text{Fe}^{\text{III}}\text{TMPyP}(\text{Im})_2^{5+}$  gives rise to the Raman bands mainly due to the  $\text{C}_\alpha\text{-N}$  and  $\text{C}_\beta\text{-C}_\beta$  stretching modes at 1374 and 1576  $\text{cm}^{-1}$ , respectively. On transformation to the ferrous porphine these bands shift to 1359 and 1572  $\text{cm}^{-1}$  (Figure 3B), respectively. As already mentioned, the ferrous high-spin complex  $\text{Fe}^{\text{II}}\text{TPP}(2\text{-CH}_3\text{Im})_2$  gives bands A and D at 1345 and 1542  $\text{cm}^{-1}$ , respectively, which are appreciably lower than the frequencies of the corresponding modes observed for the low-spin complexes; i.e., 1355–1369  $\text{cm}^{-1}$  for band A and 1560–1572  $\text{cm}^{-1}$  for band D.<sup>14,15</sup> Therefore, the feature observed for the RRS spectrum in Figure 3B conforms well to that characteristic of the ferrous porphines in a low-spin state. From Figure 3A,B it is clear that the bands, which are recognized to be core-size sensitive in the previous section, shift to the lower frequency side (1576  $\rightarrow$  1572, 1464  $\rightarrow$  1461, and 396  $\rightarrow$  387  $\text{cm}^{-1}$ ) on transformation from the ferric to ferrous state. The magnitudes of the shifts, however, are appreciably smaller than the corresponding shifts in the high-spin state (e.g., 1557  $\rightarrow$  1547, 1452  $\rightarrow$  1433, and 397  $\rightarrow$  372  $\text{cm}^{-1}$  at pH 1.0). This result suggests that the core expansion in the low-spin state is smaller than the expansion in the high-spin state.

**SERS + RRS Spectra of  $\text{Fe}^{\text{III/II}}\text{TMPyP}^{5+/4+}$ .** Parts A and B of Figure 4 represent the SERS + RRS spectra of  $1.0 \times 10^{-4}$  M  $\text{FeTMPyP}$  at pH 5.6 (in 0.1 M  $\text{Na}_2\text{SO}_4$ ) recorded at  $-0.1$  and  $-0.35$  V, respectively. From comparison of these spectra with the RRS spectra shown in Figure 2, it can be recognized that the adsorbate at  $-0.1$  and  $-0.35$  V gives rise to surface spectra that are almost identical with the RRS spectra of  $\text{Fe}^{\text{III}}\text{TMPyP}^{5+}$  and  $\text{Fe}^{\text{II}}\text{TMPyP}^{4+}$  in the bulk solutions (pH 10.5 and 1.0), respectively. Thus, the adsorbed metalloporphines at  $-0.1$  and  $-0.35$  V exist

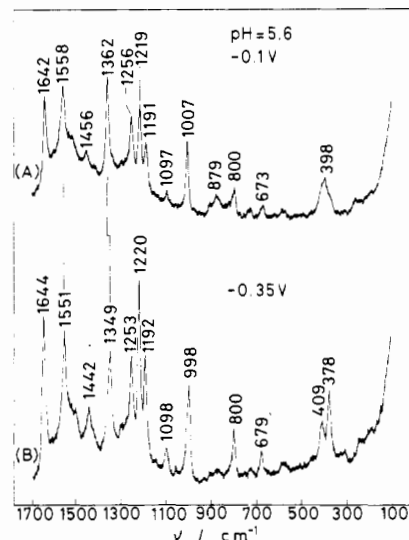


**Figure 4.** SERS + RRS spectra of  $\text{FeTMPyP}$  in 0.1 M  $\text{Na}_2\text{SO}_4$  (pH 5.6) measured at  $-0.1$  V (vs.  $\text{Ag}/\text{AgCl}$ ) (A) and at  $-0.35$  V (B) (concentration of bulk solution  $1.0 \times 10^{-4}$  M, excitation wavelength 457.9 nm).

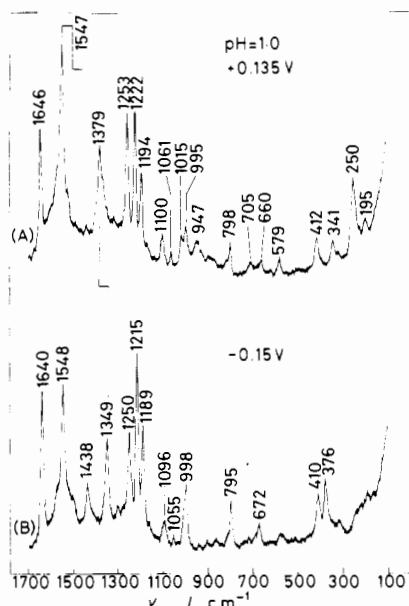


**Figure 5.** SERS + RRS spectra of  $\text{FeTMPyP}$  in 0.1 N  $\text{H}_2\text{SO}_4$  (pH 1.0) measured at  $+0.135$  V (vs.  $\text{Ag}/\text{AgCl}$ ) (A) and at  $-0.15$  V (B) (concentration of bulk solution  $1.0 \times 10^{-4}$  M, excitation wavelength 457.9 nm).

in ferric and ferrous states, respectively, and the structures of adsorbed ferric and ferrous complexes are quite similar to those of the corresponding samples in the bulk solutions. This result means that the redox reaction of the adsorbed metalloporphine at pH 5.6 proceeds in a high-spin state.

Figure 5 shows the SERS + RRS spectra of  $\text{FeTMPyP}$  observed at pH 1.0 (in 0.1 N  $\text{H}_2\text{SO}_4$ ). The surface spectrum was first observed at  $-0.15$  V after the anodization (Figure 5B), and then it was observed at  $+0.135$  V (Figure 5A). The surface spectrum recorded at  $-0.15$  V shows a feature similar to that of the RRS spectrum of the ferrous complex in 0.1 N  $\text{H}_2\text{SO}_4$  (Figure 2B), indicating that the structure taken by the ferrous complex in the solution is preserved on adsorption to the Ag electrode surface. On the other hand, as Figure 5A shows, the adsorbate at  $+0.135$  V gives a spectral feature that is quite different from those of the ferrous and ferric porphines at pH 1.0 and 10.5 (Figure 2). That is, when the electrode potential is swept from  $-0.15$  to  $+0.135$  V, the band mainly due to the  $\text{C}_\alpha\text{-N}$  stretching vibration moves to an appreciably higher frequency side (1349  $\rightarrow$  1379  $\text{cm}^{-1}$ ) while the band mainly due to the  $\text{C}_\beta\text{-C}_\beta$  stretching vibration shows only a little shift (1548  $\rightarrow$  1547  $\text{cm}^{-1}$ ). Further, the adsorbate at  $+0.135$  V gives rise to the bands at 341 and 250

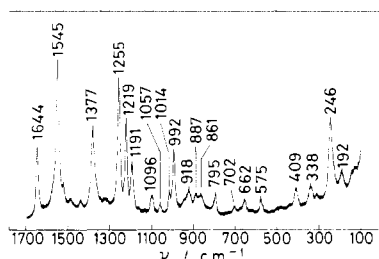
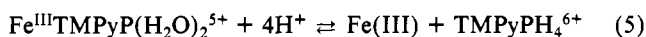


**Figure 6.** SERS + RRS spectrum of TMPyP in 1 N HCl measured at 0 V (vs. Ag/AgCl) (concentration of bulk solution  $1.0 \times 10^{-4}$  M, excitation wavelength 457.9 nm).

$\text{cm}^{-1}$ , which are absent in Figure 5B. In order to know whether the spectral change from Figure 5B to Figure 5A is arising from a change in spin state (i.e., from a high-spin state to a low-spin one), we made the SERS + RRS measurement on the sample solution ( $1.0 \times 10^{-4}$  M FeTMPyP + 0.4 M imidazole), which gives the RRS spectra shown in Figure 3. The result clearly proved that the surface spectra observed at +0.086 and -0.2 V are almost identical with the RRS spectra of  $\text{Fe}^{\text{III}}\text{TMPyP}(\text{Im})_2^{5+}$  and  $\text{Fe}^{\text{II}}\text{TMPyP}(\text{Im})_2^{4+}$  in the low-spin state (parts A and B of Figure 3), respectively. Then the characteristic feature of the SERS + RRS spectrum in Figure 5A cannot be explained by the change in the spin state.

Figure 6 shows the SERS + RRS spectrum of TMPyP ( $1.0 \times 10^{-4}$  M in 1 N HCl) measured at 0 V (The anodization in this experiment was performed at +0.1 V by the same procedure mentioned in the experimental section. After the potential was kept at -0.25 V to get the electrode surface covered by a fresh Ag layer, the potential was changed to 0 V. Although we tried to observe the surface spectrum of TMPyP in 0.1 N  $\text{H}_2\text{SO}_4$  with 457.9-nm excitation, we could not get a spectrum of high quality because of high fluorescence background.). Comparing the spectrum in Figure 6 with that in Figure 5A, we notice a remarkable similarity between these two surface spectra. A preliminary experiment indicated that the surface spectrum in Figure 6 (and the spectrum in Figure 5A) is quite similar to the RRS spectrum of TMPyP in 1 N HCl, which is considered to be in a diacid form.<sup>21</sup> Therefore, we can conclude from Figure 5 that sweeping the electrode potential from -0.15 to +0.135 V causes a complete release of the central iron atom of the adsorbed metalloporphine, leaving the ligand in the diacid form. A cyclic voltammetry measurement, which was performed on FeTMPyP in 0.1 N  $\text{H}_2\text{SO}_4$  by using the same electrochemical cell as that used for the measurement of the SERS + RRS spectra in Figure 5, indicated that redox reaction of the metalloporphine proceeds with the half-wave potential of -0.012 V (The difference of this value that reported by Forshey and Kuwana<sup>10</sup> can be ascribed to the fact that the Ag working electrode was used in the present study while a gold working electrode was employed in the study of Forshey and Kuwana.). Then, the oxidation of the central iron atom of the ferrous complex should precede the demetalization process, which can be expressed as



As already mentioned, the RRS spectrum shown in Figure 2A clearly proves that this reaction does not occur in the 0.1 N  $\text{H}_2\text{SO}_4$  solution of the ferric porphine. In the bulk solution water molecules surround the diaquo ferric porphine, which probably prevents the access of hydrogen ions to the complex. On the other hand, at the Ag electrode surface the adsorbed ferric porphine, which exists in an inner Helmholtz layer, becomes partially hy-

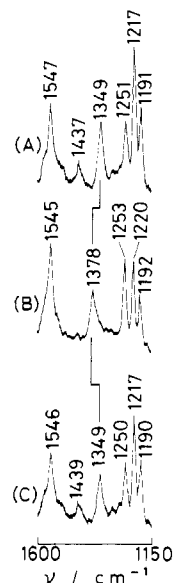


**Figure 7.** SERS + RRS spectra of FeTMPyP in 0.1 N  $\text{H}_2\text{SO}_4$  observed by sweeping the electrode potential to -0.15 (A), +0.135 (B), and -0.15 V (C), successively (see text; concentration of bulk solution  $1.0 \times 10^{-4}$  M, excitation wavelength 457.9 nm).

drated and can readily be attacked by the hydrogen ions. When  $\text{Na}_2\text{SO}_4$  was added to increase the ionic strength of the sample solution at pH 1.0, the observed SERS + RRS spectra at +0.135 V gave rise to the bands due to the ferric complex in the high-spin state in addition to the bands due to the porphine in the diacid form. Presumably the addition of  $\text{Na}_2\text{SO}_4$  reduces the electrostatic interaction between the ferric porphine and the electrode surface, which suppresses the conversion of the complex to the porphine in the diacid form. In order to elucidate further the reaction processes of eq 1 and 5, which are considered to take place at the Ag electrode surface in the 0.1 N  $\text{H}_2\text{SO}_4$  solution of the metalloporphine, we performed the following experiments. After we measured the SERS + RRS spectrum at +0.135 V shown in Figure 5A, we completely replaced the sample solution with 0.1 N  $\text{H}_2\text{SO}_4$  and changed the electrode potential back to -0.15 V. Figure 7A represents the surface spectrum in the 1600-1150- $\text{cm}^{-1}$  region at -0.15 V, which is almost identical with that of the ferrous porphine shown in Figure 5B. Then the potential was swept again to +0.135 V and the surface spectrum was recorded, the result being shown in Figure 7B. This spectrum gives a feature quite similar to that observed in Figure 5A. Finally, the surface spectrum was again obtained at -0.15 V as shown in Figure 7C. The last spectrum is almost identical with that in Figure 7A. From these experiments we can conclude as follows: (i) when the electrode potential is changed between -0.15 and +0.135 V, the reactions of eq 1 and 5 proceed almost reversibly at the Ag electrode surface in the 0.1 N  $\text{H}_2\text{SO}_4$  solution of the metalloporphine and (ii) the ferric ion, which is released from the ferric porphine around +0.135 V, does not diffuse out of the Helmholtz layer and is recombined with the porphine around -0.15 V, resulting in the formation of the ferrous monoquo porphine. Although the mechanism of interaction that fixes the ferric ion near the porphine is still unknown, the experimental results reveal a new aspect of the reaction process that the metalloporphine undergoes at the electrode surface.

**Registry No.**  $\text{Fe}^{\text{III}}\text{TMPyP}(\text{H}_2\text{O})_2^{5+}$ , 82091-95-0;  $\text{Fe}^{\text{III}}\text{TMPyP}(\text{OH})_2^{3+}$ , 75908-34-8;  $[\text{Fe}^{\text{III}}\text{TMPyP}(\text{H}_2\text{O})]_2\text{O}^{8+}$ , 75908-35-9;  $\text{Fe}^{\text{II}}\text{TMPyP}(\text{OH})^{3+}$ , 98875-83-3;  $\text{Fe}^{\text{II}}\text{TMPyP}(\text{H}_2\text{O})^{4+}$ , 97878-29-0;  $\text{Fe}^{\text{III}}\text{TMPyP}(\text{Im})_2^{5+}$ , 72595-74-5;  $\text{Fe}^{\text{II}}\text{TMPyP}(\text{Im})_2^{4+}$ , 87306-61-4; Ag, 7440-22-4; Fe, 7439-89-6.

(21) Neri, B. P.; Wilson, G. S. *Anal. Chem.* **1972**, *44*, 1002.